Synthesis and Self-Assembly in Bulk of Linear and Mikto-Arm Star Block Copolymers Based on Polystyrene and Poly(glutamic acid)

Jérôme Babin,[†] Daniel Taton,*[,†] Martin Brinkmann,[‡] and Sébastien Lecommandoux*[,†]

Laboratoire de Chimie des Polymères Organiques, CNRS, ENSCPB-Université Bordeaux 1, 16 Avenue Pey Berland, 33607 PESSAC, France, and Institut Charles Sadron, CNRS, UPR 22, 6 Rue Boussingault BP 40016 F-67083 Strasbourg Cedex, France

Received September 14, 2007; Revised Manuscript Received December 5, 2007

ABSTRACT: Both AB linear-type and AB_2 miktoarm star-type amphiphilic block copolymers based on polystyrene (PS) as A block and poly(glutamic acid) (PGA) as B block were obtained by a four-step synthetic approach combining (i) atom transfer radical polymerization of styrene and (ii) chemical modification of the bromo end groups of ATRP-derived precursors into many or twice as many primary amino groups, followed by (iii) ring-opening polymerization of γ-benzyl-L-glutamate *N*-carboxyanhydride and (iv) a final step of hydrolysis. The self-assembly properties in bulk of these linear PS-*b*-PGA and miktoarm star PS-*b*-$(PGA)_2$ block copolymers were subsequently investigated by different analytical means, including Fourier transform infrared spectroscopy (FTIR), wide and small-angle X-ray scattering (WAXS and SAXS) and atomic force microscopy (AFM). FTIR analysis revealed that the PGA block systematically adopted a rodlike α-helix conformation, even for degree of polymerization as low as 18. The very high immiscibility between PS and PGA blocks (conformational asymmetry) drove all of these rod−coil block copolymers to self-assemble in a hexagonal in lamellar (HL) morphology in the nanometer size range, whatever their composition and architecture. In addition, WAXS and SAXS results evidenced the effect of the macromolecular architecture on the local organization of PGA helices: the linear block copolymers showed an internal lamellar structure with PGA helices stacked, inter-digitated or folded depending on the weight fraction of the rodlike PGA blocks, whereas miktoarm stars exhibited a stacked microstructure, independently of the PGA content.

Introduction

Block copolymers find miscellaneous applications owing to their self-assembly properties in bulk or in selective solvents, giving rise to a wide range of morphologies in the submicrometer size range (spherical or cylindrical micelles, vesicles, lamellae, etc.).[1−6] These properties make block copolymer materials useful as compatibilizing additives, viscosity modifiers, stabilizers of colloidal suspensions, nanocarriers for the encapsulation and controlled release of drugs, templates for mineralization, or supports for homogeneous catalysis.[1−10] For linear block copolymers where each block adopts a coil conformation, the shape and size of morphologies depend on three parameters, including (1) the total degree of polymerization N of the block copolymer, (2) its overall composition, and (3) the thermodynamic interaction between the two blocks which is expressed by the dimensionless Flory−Huggins interaction parameter χ_{AB} (or χ). On the basis of these parameters, experimental[1,2] and theoretical[3−5] phase diagrams have been successfully established, some of these "coil−coil" block copolymers being practically used as materials in nowadays life. The phase diagram of coil−coil copolymers is also determined by the conformational asymmetry between the two blocks. One can either induce this asymmetry in one block which would exhibit a conformation distinct from a coil, or introduce branching points to perturb the conformational entropy of copolymer chains. The former case corresponds typically to rod−dendrons[11,12] and rod−coils[13,14] while the latter case embraces block copolymers with branched architectures, e.g., cyclic copolymers,[15−17] star−block copolymers,[18,19] dendrimer-like copolymers,[20] or graft copolymers.[21] For instance, it has been demonstrated both theoretically[22] and experimentally[23] that rod−coil block copolymers undergo a phase separation at the length scale of a few nanometers because of a higher incompatibility between the blocks, as compared to coil−coil copolymers where phase separation typically occurs on larger characteristic length scale. Unique and non-predicted morphologies based on rod−coil systems were found, which include the "mushroom-like structure" described by Stupp and colleagues,[24] the "zigzag morphology" reported by Thomas and colleagues,[25] the "microporous morphology" observed by Jenekhe and colleagues,[26] or the "hexagonal in lamellar" or "double hexagonal assemblies" of polypeptide-based copolymers reported by different teams.[27−36] On the other hand, it is now well documented that block copolymers with a branched architecture bring about self-assembled organizations which are distinct from those observed with linear counterparts.[37,38] In this regard, block copolymers with a star-shaped architecture are well suited for investigations into the structure−property relationships of branched polymers, since possessing only one branching point per macromolecule.[37,38] One can distinguish between star-block copolymers for which the presence of a single junction for all the diblock arms results in a core−shell structure, and miktoarm or heteroarm star copolymers containing either chemically different arms or multiple arms with variable sizes. Specifically, the theoretical phase behavior of coil−coil A_nB miktoarm stars has been first addressed by Milner and col.[39] in the strong segregation limit and, more recently, by Grason et al.[40] in the weak and intermediate segregation limit. These models have been successfully confirmed by experimental studies realized by Gido

* Corresponding authors. E-mail: taton@enscpb.fr (D.T.) and lecommandoux@enscpb.fr (S.L.). Telephone: 33-540-008486. Fax: 33-540-008487.

† Laboratoire de Chimie des Polymères Organiques, CNRS, ENSCPB-Université Bordeaux 1.

‡ Institut Charles Sadron, CNRS, UPR 22.

10.1021/ma702071y CCC: $40.75
Published on Web 01/25/2008

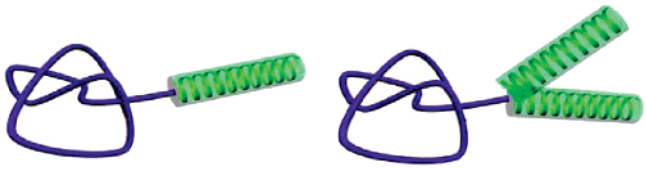

Figure 1. Representation of rod−coil block copolymer architectures: linear diblock PS-*b*-PGA (left) and three-arm miktoarm star PS-*b*-$(PGA)_2$ (right).

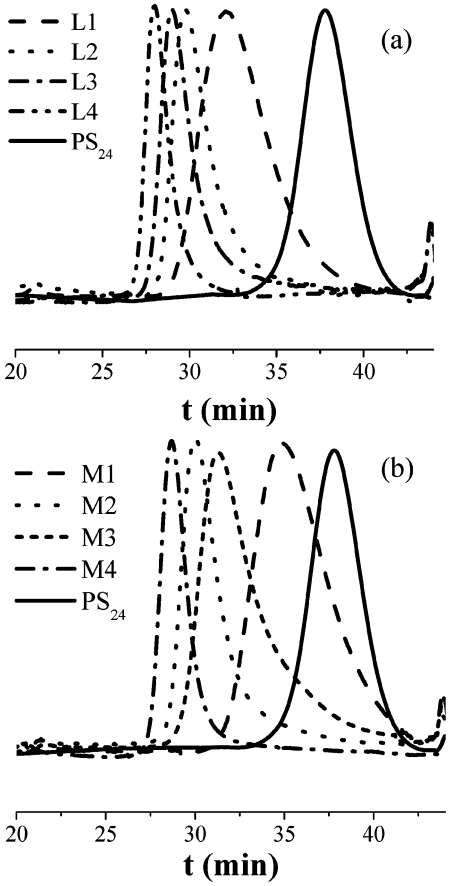

Figure 2. SEC chromatograms (DMF/LiBr 60 °C, refractive index detector) of PS-*b*-PBLG linear diblocks: (a) PS-*b*-$(PBLG)_2$ miktoarm stars (b) and macroinitiator PS_{24}.

and col.[41] on A_2B, A_3B, and A_5B miktoarm stars, where A and B are the poly(isoprene) and the polystyrene blocks respectively, the couple of blocks showing a negligible conformational asymmetry.

In the present work, both the effect of the conformational asymmetry and the presence of branching points on the self-assembly in bulk of block copolymers are examined. For that purpose, well-defined rod−coil block copolymers comprising one polystyrene (PS) B block and one (AB) or two (A_2B) poly(L-glutamic acid) (PGA) A blocks have been designed. This was achieved following a straightforward four-step synthetic strategy which combines atom transfer radical polymerization of styrene, selective derivatization of PS chain-ends, ring-opening polymerization of γ-benzyl-L-glutamate *N*-carboxyanhydride, and final treatment under acidic conditions. In both types of block copolymers (see Figure 1), the PS blocks adopt a coil (or wormlike chains due to their short length) conformation whereas the PGA blocks exhibit a α-helical conformation and behave as rigid rods. We present here the thorough structural characterization of nanosize range morphologies formed by self-assembly in bulk, from films of these block copolymers obtained by slow solvent evaporation, as a function of their composition and architecture.

Experimental Section

Materials. Styrene (99%), dichloromethane (CH_2Cl_2, 99%), tetrahydrofuran (THF, 99%) and *N*,*N*-dimethylformamide (DMF, 99%) were stirred overnight over CaH_2 and distilled under reduced pressure prior to use. γ-Benzyl-L-glutamate (Bz-L-GluNCA) was dried after crystallization from hexane and kept under argon in a glovebox. Copper(I) bromide (CuBr, 98%), (1-bromoethyl)benzene (97%), ethylenediamine (98%), 1-aminotriethylenetriamine (96%), hydrogen bromide (HBr, 33 wt %), trifluoroacetic acid (TFA, 99%), and 2,2′-bipyridyl (bipy, 99%) were used as received. All reagents were purchased from Aldrich.

Synthesis of Linear PS-*b*-PGA (L1-L4) and Miktoarm Star PS-*b*-PGA_2 (M1-M4) Block Copolymers. All polymerizations were carried out in a Schlenk flask equipped with a magnetic bar that was first flamed and dried under vacuum. Monomer conversion was determined by gravimetry. Samples referred to as $PS(NH_2)_2$ and PS-*b*-$(PGA)_2$ (see Scheme 1) were synthesized as described previously in ref 42.

Synthesis of ω-Bromopolystyrene, PS(Br), by Atom Transfer Radical Polymerization. In a typical experiment, a Schlenk flask was charged with 2.48 g (1.73×10^{-2} mol) of CuBr, 5.42 g (3.46×10^{-2} mol) of bipy, 8 mL of DMF, 2.36 mL (1.73×10^{-2} mol) of phenyl ethyl bromide, and 80 mL (0.69 mol) of styrene under N_2 atmosphere. The reaction mixture was degassed by three freeze−pump−thaw cycles, back-filled with N_2 and placed in an oil bath thermostated at 100 °C. After 120 min, the flask was cooled with liquid nitrogen and the contents were diluted with CH_2Cl_2. The reaction mixture was passed through a column of neutral alumina to remove the copper salts. The polymer was precipitated twice into a large excess of methanol, filtered, and dried at 50 °C under vacuum for 24 h. Monomer conversion: 60%. ^{1}H NMR ($CDCl_3$) δ (ppm): 7.3−6.3 (m, 5H aromatic), 4.5 (broad s, 1H, C*H*(ph)−Br), 2.2−1.2 (m, aliphatic main chain), 1 (m, CH_3 initiator). SEC (DMF): $M_n = 2450$ g mol^{-1}, $M_w/M_n = 1.08$.

Synthesis of ω,ω′-bis(amino)polystyrene, $PS(NH_2)_2$. PS(Br) (12 g, 4.6×10^{-3} mol, $M_n = 2600$ g mol^{-1}, $M_w/M_n = 1.08$) was dissolved in dry DMF (100 mL), and 21 mL (0.147 mol) of tris(2-aminoethyl)amine was added. After the reaction was stirred for 5 days at room temperature, the excess triamine was removed by phase transfer of the polymer in cyclohexane. Analysis by thin layer chromatography (SiO_2:CH_2Cl_2) showed that the crude product contained residual PS(Br). These PS(Br) chains were removed by selective precipitation as follows: the reaction mixture was dissolved in cyclohexane and ten drops of concentrated HCl (35%) were added. Hexane was then added slowly to the former solution until precipitation of the quaternized amine PS. The polymer was dissolved with dichloromethane and extracted three times with a saturated K_2CO_3 water solution. The organic phase was separated, dried over magnesium sulfate, filtered, and evaporated to dryness. Finally, precipitation in methanol and vacuum drying at 40 °C afforded the $PS(NH_2)_2$ (yield: 78%). ^{1}H NMR ($CDCl_3$) δ (ppm): 7.3−6.3 (m, 5H aromatic), 3.2−3 (broad, 1H, C*H*-NH), 2.7−2.5 (m, 4H, 2 × CH_2NH$_2$), 2.5−2.2 (m, 8H, 2 × CH_2CH$_2$NH$_2$ and NHCH_2CH_2N), 2.2−1.2 (m, aliphatic main chain), 1 (m, CH_3 initiator). SEC (DMF): $M_n = 2360$ g mol^{-1}, $M_w/M_n = 1.08$.

Synthesis of ω-aminopolystyrene, $PS(NH_2)$. The synthesis of $PS(NH_2)$ was achieved following a similar procedure using a large excess of ethylenediamine as a functionalizing agent (Scheme 1). ^{1}H NMR ($CDCl_3$) δ (ppm): 7.3−6.3 (m, 5H aromatic), 3.2−3 (broad, 1H, C*H*-NH), 2.7−2.5 (m, 2H, CH_2NH$_2$), 2.5−2.2 (m, 2H, CH_2CH$_2$NH$_2$), 2.2−1.2 (m, aliphatic main chain), 1 (m, CH_3 initiator). SEC (DMF): $M_n = 2390$ g mol^{-1}, $M_w/M_n = 1.07$.

Synthesis of Miktoarm Polystyrene-*b*-poly(γ-benzyl-L-glutamate) Star Block Copolymers, PS-*b*-$(PBLG)_2$ by Ring-Opening Polymerization from $PS(NH_2)_2$. In a typical experiment, Bz-L-GluNCA (3.26 g, 1.24×10^{-2} mol) was weighed in a glovebox, introduced into a Schlenck flask, and dissolved with

Scheme 1. Synthetic Pathway to Linear PS-*b*-PGA and Miktoarm Star PS-*b*-(PGA)$_2$ Block Copolymers

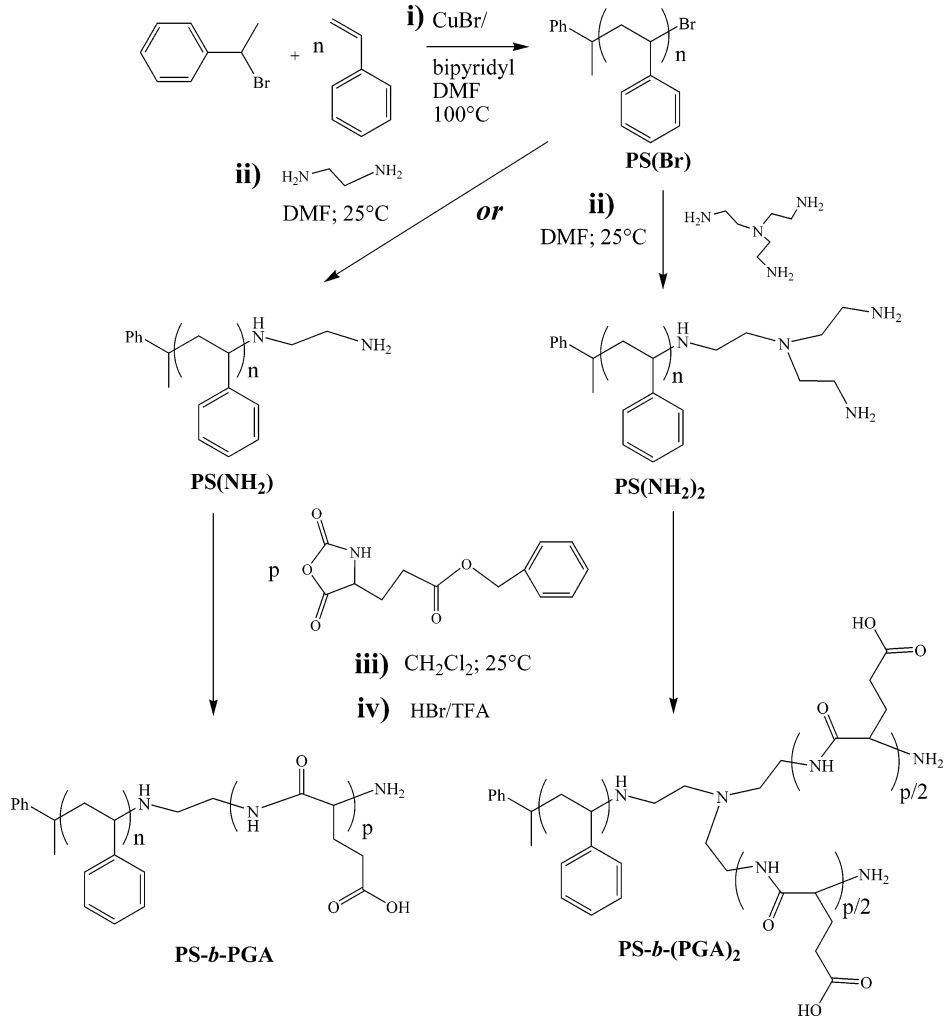

anhydrous CH_2Cl_2 (23 mL). In a separate flask, the PS$(NH_2)_2$ macroinitiator (0.45 g, 1.77×10^{-4} mol) was dissolved with dry CH_2Cl_2 (10 mL) and added via cannula. The solution was degassed and stirred for 24 h at room temperature. The copolymer was recovered by precipitation in diethyl ether and dried under vacuum. Monomer conversion and overall yield were 97%. ^{1}H NMR ($CDCl_3$, TFA: 80, 20) δ (ppm): 8.1−7.8 (m, 1H, CHN*H*CO), 7.5−6.3 (m, 5H aromatic), 5.3−5 (m, 2H, CH_2−Ph), 4.7−4.5 (m, 1H, C*H*NH-CO), 2.7−1.2 (m, aliphatic main chain), 1 (m, CH_3 initiator).

Synthesis of Linear Polystyrene-*b*-poly(γ-benzyl-L-glutamate) Block Copolymers, PS-*b*-PBLG by Ring-Opening Polymerization from PS$(NH_2)_2$. The synthesis of PS-*b*-PBLG was achieved following a similar procedure. ^{1}H NMR ($CDCl_3$, TFA: 80, 20) δ (ppm): 8.1−7.8 (m, 1H, CHN*H*CO), 7.5−6.3 (m, 5H aromatic), 5.3−5 (m, 2H, CH_2−Ph), 4.7−4.5 (m, 1H, C*H*NHCO), 2.7−1.2 (m, aliphatic main chain), 1 (m, CH_3 initiator).

Synthesis of Amphiphilic Linear PS-*b*-PGA (L1-L4) and Miktoarm Star PS-*b*-(PGA)$_2$ (M1-M4) Block Copolymers. In a typical experiment, PS-*b*-(PBLG)$_2$ (0.8 g, M_n = 18 500 g mol^{-1}, 4.32×10^{-5} mol) was dissolved in TFA (8 mL). Then HBr/acetic acid, 33 wt %, (3 mL, 1.55×10^{-2} mol) was added, and the mixture was stirred at room temperature for 1 h. The polymer was precipitated by addition of diethyl ether, filtered, and washed with distilled water to remove HBr. The powder was dried under vacuum for 48 h. ^{1}H NMR (DMSO-d_6) δ (ppm): 10.2−9.6 (broad, COO*H*), 8.5−7.8 (broad, 1H, CHN*H*CO), 7.3−6.3 (m, 5H aromatic), 4.4−3.7 (m, 1H, C*H*NHCO) 2.7−1.2 (m, aliphatic main chain), 1 (m, CH_3 initiator) (see Figure 3).

Characterization. ^{1}H NMR spectra were recorded at room temperature on a Bruker AC 400 spectrometer in $CDCl_3$ for PS-*b*-(PBLG)$_{n=1;2}$ and DMSO-d_6 for PS-*b*-(PGA)$_{n=1;2}$. Molar masses distributions were determined by size exclusion chromatography (SEC) with *N*,*N*′-dimethylformamide (DMF) as eluent (1 mL/min) at 60 °C with LiBr, equipped with a refractive index detector (Jasco, RI-1530), and three columns TSK (8 × 300 mm, 5 μm, G2000, G3000, G4000 HHR). SEC was calibrated using linear polystyrene samples. FTIR spectra were recorded at room temperature on a BRUKER Tensor 37 spectrometer in the spectral range of 650−4000 cm^{-1}. Samples were prepared by drop-casting a thin film from a diluted DMF-solution onto a reflection ATR cell. Small and wide-angle X-ray scattering (SAXS and WAXS) experiments were performed using Cu Kα radiation (1.54 Å wavelength) using a Nanostar from Bruker AXS (operating at 40 kV, 35 mA). A CCD detector (Siemens Hi-Star), at a sample to detector distances of 23 or 106.2 cm, was used to record scattering patterns. The accessible wave vector (q) range was 0.01 Å^{-1} < q < 2 Å^{-1}. The surface morphology of the samples was investigated by Atomic Force Microscopy (AFM) on a Nanoscope III in tapping mode using Si tips (25−50 N/m and 280−365 kHz). The flat and neat surfaces of the bulk copolymer samples were prepared by using a Leica Ultracut S microtome with a FCS cryo-temperature attachment and a Diatome diamond knife at −80 °C.

Specimen's Preparation. Copolymer films with an average thickness of 400 μm were prepared by slow evaporation from 10 wt % DMF mixtures in Teflon molds. Dynamic light scattering measurements at 90° have confirmed the molecular dissolution of copolymers in DMF (R_H < 5 nm) prior to film formation. After 1 week of casting, solvent residues were removed under vacuum at room temperature. Because of the presence of side carboxylic acid

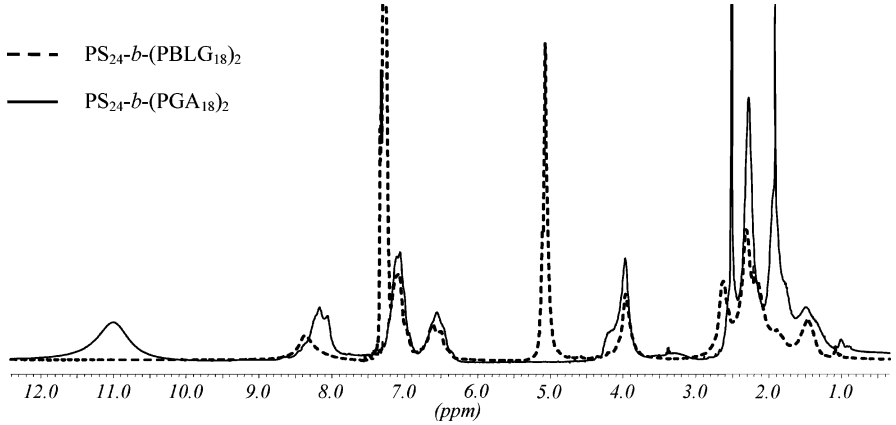

Figure 3. ^{1}H NMR of PS_{24}-*b*-$(PBLG_{18})_2$ ($CDCl_3$) and PS_{24}-*b*-$(PGA_{18})_2$ (DMSO-d_6) after deprotection.

Table 1. Molecular Characteristics of Linear PS-*b*-PGA and Miktoarm Star PS-*b*-$(PGA)_2$ Copolymers

	composition	sample	$\overline{M}_{nPS}$ (g mol^{-1})[a]	$\overline{DP}_{PS}$[a]	$\overline{M}_{nPGA}$ (g mol^{-1})[b]	$\overline{DP}_{PGA}$[b]	$\overline{M}_{ncopo}$ (g mol^{-1})	PDI[c]	ϕ_{PGA} (% mol)
linear	PS_{24}-*b*-PGA_{36}	L1	2600	24	4650	36	7250	1.22	64
	PS_{24}-*b*-PGA_{76}	L2	2600	24	9800	76	12 400	1.10	79
	PS_{24}-*b*-PGA_{104}	L3	2600	24	13 410	104	16 010	1.09	84
	PS_{24}-*b*-PGA_{138}	L4	2600	24	17 800	138	20 400	1.13	87
miktoarm	PS_{24}-*b*-$(PGA_{18})_2$	M1	2600	24	4770	37	7370	1.26	65
	PS_{24}-*b*-$(PGA_{36})_2$	M2	2600	24	9300	72	11 900	1.14	78
	PS_{24}-*b*-$(PGA_{51})_2$	M3	2600	24	13 160	102	15 760	1.15	83
	PS_{24}-*b*-$(PGA_{71})_2$	M4	2600	24	18 300	142	20 900	1.16	88

[a] Determined by SEC (60 °C, DMF + LiBr, 1 mL/min, PS standard). [b] Determined before deprotection by ^{1}H NMR in $CDCl_3$ knowing the molecular weight of the PS-based macroinitiator as determined by SEC. [c] Polydispersity index, determined before deprotection by SEC (60 °C, DMF + LiBr, 1 mL/min, PS standard).

groups in PGA blocks, no further heat treatment was carried out to avoid the possible degradation of the copolymer.[43]

Results and Discussion

Synthesis of Linear PS-*b*-PGA (L1-L4) and Miktoarm Star (M1-M4) PS-*b*-PGA_2 Block Copolymers. To access both AB linear-type and AB_2 miktoarm star-type block copolymers based on PS and PGA, we developed a straightforward four-step synthetic approach. We already reported the synthesis of miktoarm stars but not yet that of the linear counterparts.[42] Briefly, our method (see Scheme 1) combines (i) atom transfer radical polymerization (ATRP) of styrene and (ii) chemical modification of the ω-bromo end groups of PS chains derived by ATRP into one or two primary amino groups, followed by (iii) ring-opening polymerization (ROP) of γ-benzyl-L-glutamate *N*-carboxyanhydride (Bz-L-GluNCA), and (iv) a final step of hydrolysis. Recent reports also showed how to combine ATRP and ROP of *N*-carboxyanhydrides[44] to derive either linear or star-block copolymers;[45−52] this is part of the review article by Haddleton and colleagues.[53] The first step (i) thus consisted in the synthesis of ω-bromo-PS by ATRP of styrene using CuBr/bipy as catalytic system in the presence of DMF as additive and 1-phenylethyl bromide as initiator. Under these conditions, good control over the molar masses, polydispersities, and functionalities could be achieved (Table 1). The next step (ii) involved the preparation of both PS chains fitted with one ω- or two geminal ω,ω'-amino groups, $PS(NH_2)$ and $PS(NH_2)_2$, respectively. This was accomplished by nucleophilic displacement of the bromo end groups of PS(Br), using a large excess (30 equiv) of ethylenediamine and 1-aminotriethylenetriamine, respectively, in DMF. Nonfunctionalized PS chains could be easily removed by selective precipitation in hexane after treatment of $PS(NH_2)$ and $PS(NH_2)_2$ with aqueous HCl (see Experimental Section). Chemical purity of each compound was checked by ^{1}H NMR. The poly(γ-benzyl-L-glutamate) (PBLG) arms were subsequently grown step (iii) by ROP of Bz-L-GluNCA from these $PS(NH_2)$ and $PS(NH_2)_2$ macroinitiators using CH_2Cl_2 as solvent at 25 °C. Size exclusion chromatography (SEC) analysis showed the total disappearance of PS signal both for the synthesis of linear and miktoarm star block copolymers, indicating a quantitative initiation from the corresponding macroinitiators (Figure 2). In addition, narrow molecular weight distributions denoted high control of the polymerization process. In these conditions the length of PBLG blocks could be varied from the ratio $[M]_0/[A]_0$ (with $[M]_0$ and $[A]_0$ are the initial concentrations of monomer and macroinitiator, respectively). The last step (iv) to the targeted PS-*b*-PGA and PS-*b*-$(PGA)_2$ block copolymers consisted in the cleavage of the benzyloxycarbonyl groups with an excess of hydrogen bromide in trifluoroacetic acid. The total disappearance of the protecting group signals (δ = 7.3 ppm of $CH_2-\underline{Ph}$ and δ = 5 ppm of C $\underline{H_2}$−Ph) in the ^{1}H NMR spectra confirmed the efficacy of the deprotection step (Figure 3). The molecular characteristics of the amphiphilic linear and miktoarm star block copolymers, denoted L1−L4 and M1−M4 respectively, are summarized in Table 1. Because SEC experiments were performed using a refractive index detector calibrated with linear PS standards, the molecular weight extracted from chromatograms of Figure 2 could not be used quantitatively. A more reliable value of molecular weight was determined by ^{1}H NMR before deprotection using the signal of the PS block as reference. In order to carefully explore an important part of the phase diagram, we synthesized a set of well-defined block copolymers for each type of architectures, with a molar fraction of PGA varying from 64% to 88%. It is noteworthy that linear and miktoarm star samples consisted of the same composition and molecular weight, facilitating the comparison of their self-assembly properties in bulk.

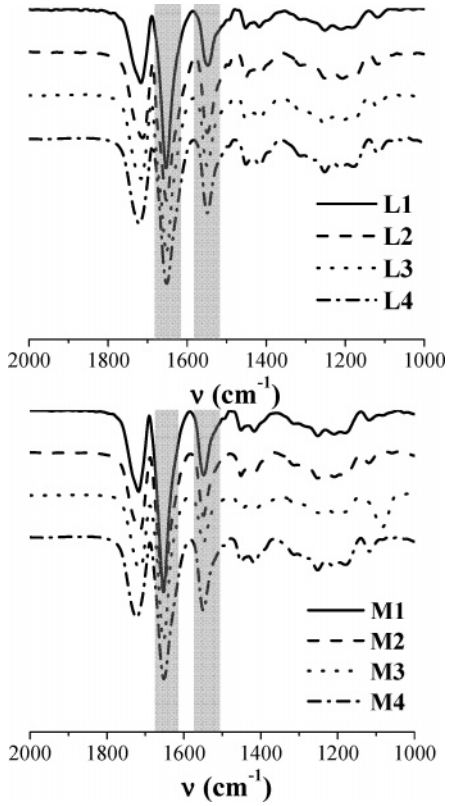

Figure 4. FTIR-spectra of PS-*b*-PGA and PS-*b*-$(PGA)_2$ copolymers. The amide bands indicative for the secondary structure of the peptide block are marked with shaded bars.

Self-Assembly in Bulk. Effects of both the conformational asymmetry (size of the rigid PGA block) and the architecture (linear or star) on the supramolecular organization of block copolymers based on PS and PGA were investigated. This was achieved using different analytical means, including Fourier transform infrared spectroscopy (FTIR), wide- and small-angle X-ray scattering (WAXS and SAXS) and atomic force microscopy (AFM).

First, conformation of the PGA blocks in these copolymers was investigated by FTIR. Peaks due to the stretching of the C═O bond (amide I) and to the deformation and stretching of the N−H bond (amide II) of the polypeptidic backbone are widely used to establish the secondary structure of polypeptides.[54,55] Typically, absorption at 1655 (amide I) and 1550 cm^{-1} (amide II) is indicative of a right-handed α-helix, while peaks at 1668 and 1556 cm^{-1} are characteristics of a left-handed α-helix. Position of the amide I band for parallel β-sheet is in the range 1636−1640 cm^{-1} and shifts then to 1622−1632 cm^{-1} for the antiparallel β-sheet and to 1660−1664 cm^{-1} for random-coil conformations.[56] Figure 4 shows the FTIR spectra for all PS-*b*-PGA and PS-*b*-$(PGA)_2$ block copolymers at 25 °C between 1000 and 2000 cm^{-1}. Independent of the molecular weight of the PGA block and of the architecture of the block copolymers, only amide I and amide II bands, respectively, at 1655 and 1550 cm^{-1} are observed, which is consistent with a right-handed α-helix conformation. Even for miktoarm star M1 bearing the shortest PGA arms (18 monomer units in average), no β-sheet structure is evidenced. It has been reported that a minimal chain length of 18 monomer units is required to generate stable α-helix conformation from oligopeptides.[57,58] However, recent reports have shown that attachment of a synthetic PS block to PBLG—which is hydrophobic compared to PGA—can significantly stabilize the α-helical secondary polypeptidic segment if the latter possesses less than 20 monomer units.[28,29] Our findings thus show that the hydrophilic PGA block better stabilize the α-helical confirmation in bulk than PBLG, all copolymers being of rod−coil type.

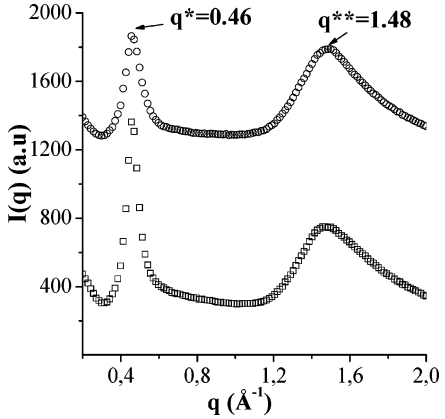

Figure 5. WAXS patterns from linear diblock PS_{24}-*b*-PGA_{104} (L3, circle) and miktoarm star PS_{24}-*b*-$(PGA_{51})_2$ (M3, square) copolymers.

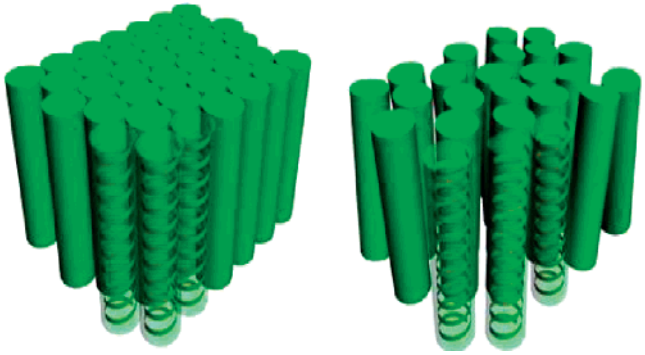

Figure 6. Representation of the hexagonal arrangement of PGA helices: ordered (left), disordered (right).

In order to account for the local organization of the polypeptidic α-helices, films were prepared from solvent casting and WAXS experiments were performed at room temperature over the scattering vector region $0.2 < q < 2$ $Å^{-1}$. Figure 5 shows one-dimensional WAXS data obtained for miktoarm star copolymer M3 and linear diblock analogue L3 possessing the same composition and molecular weight. All copolymers exhibited similar scattering intensity profiles, with two main scattering peaks. The first peak at $q^* = 0.46$ $Å^{-1}$ can be attributed to the first reflection of the set of Bragg peaks with ratio $1:\sqrt{3}:\sqrt{4}$ characteristic of the columnar hexagonal packing of polypeptides in α-helix conformation.[27,28,33,36,59−61] However, the rather large width of this peak at q^* and the absence of the higher-order Bragg reflections $\sqrt{3}$ and $\sqrt{4}$ indicate a poor ordering of the PGA helices. This is consistent with many other rod−coil systems based on polypeptides,[27,58,59,61] for which higher order Bragg peaks are rarely evidenced at room temperature. Only subsequent annealing at temperature >120 °C in the liquid-crystalline phase can improve the level of ordering. Unfortunately, annealing was not possible with our samples owing to the presence of carboxylic acid side groups of the PGA block which might have degraded the block copolymers, as already reported.[43]

Figure 6 illustrates the hexagonal packing of PGA helices in a well ordered paracrystalline form C (after annealing above 120 °C) and for the low level of ordering present in our samples (without annealing). On the basis of the width of the peak q^* and using the Scherrer equation,[62] a correlation length of 30 nm was determined which fits with only 20 helices in an ordered domain. The lattice of the hexagonal array corresponding to

Table 2. Morphological Characteristics for Films of Linear and Miktoarm Star Copolymers

		local structure		main structure								
	entry	*a*	d_α (Å)[b]	*a*	d_{Lam} (Å)[c]	d_{PGA} (Å)[d]	d_{PS} (Å)[e]	L_{PGA} (Å)[f]	L_{PS} (Å)[g]	L_{tot} (Å)[h]	γ[i]	global structure
linear	L1	H	16	L	153	115	38	54	26	80	1.0	HL[j]
	L2	H	16	L	209	181	28	114	26	140	1.4	HL
	L3	H	16	L	224	201	23	156	26	182	1.7	HL
	L4	H	16	L	299	275	24	207	26	233	1.7	HL
miktoarm	M1	H	16	L	108	65	43	27	26	53	0.9	HL[j]
	M2	H	16	L	185	139	46	54	26	80	0.9	HL
	M3	H	16	L	203	165	38	77	26	103	1.0	HL
	M4	H	16	L	267	229	38	107	26	133	1.0	HL

[a] Key: H, hexagonal structure; L, lamellar structure. [b] Spacing between PGA α-helix $d_\alpha = 4\pi/q^*\sqrt{3}$. [c] Lamellar periodicity $d_{lam} = 2\pi/q^*$. [d] PGA domain spacing $d_{PGA} = d_{lam}(1 + \phi_{PS}\nu_{PS}/\phi_{PGA}\nu_{PGA})^{-1}$, with ϕ_I the weight fraction and ν_I the specific volume: $\nu_{PS} = 0.95$ cm^3 × g^{-1}, $\nu_{PGA} = 1.55$ cm^3 × g^{-1}. [e] PS domain spacing $d_{PS} = d_{lam}$ - d_{PGA}. [f] Maximum length of PGA in α-helix $L_{PGA} = 1.5DP_{PGA}/n$, with *n* the number of arms. [g] Length of PS in statistical conformation $L_{PS} = 2\sqrt{(0.0724M_{n,PS})}$. [h] Total theoretical length $L_{tot} = L_{PGA} + L_{PS}$. [i] Geometrical factor $\gamma = (8 \times 10^{24}/\pi N_A)(M_n/\rho d_{lam} d_\alpha)$, with N_A Avogadro's constant and ρ average density. [j] HL indicates "hexagonal in lamellar" morphology.

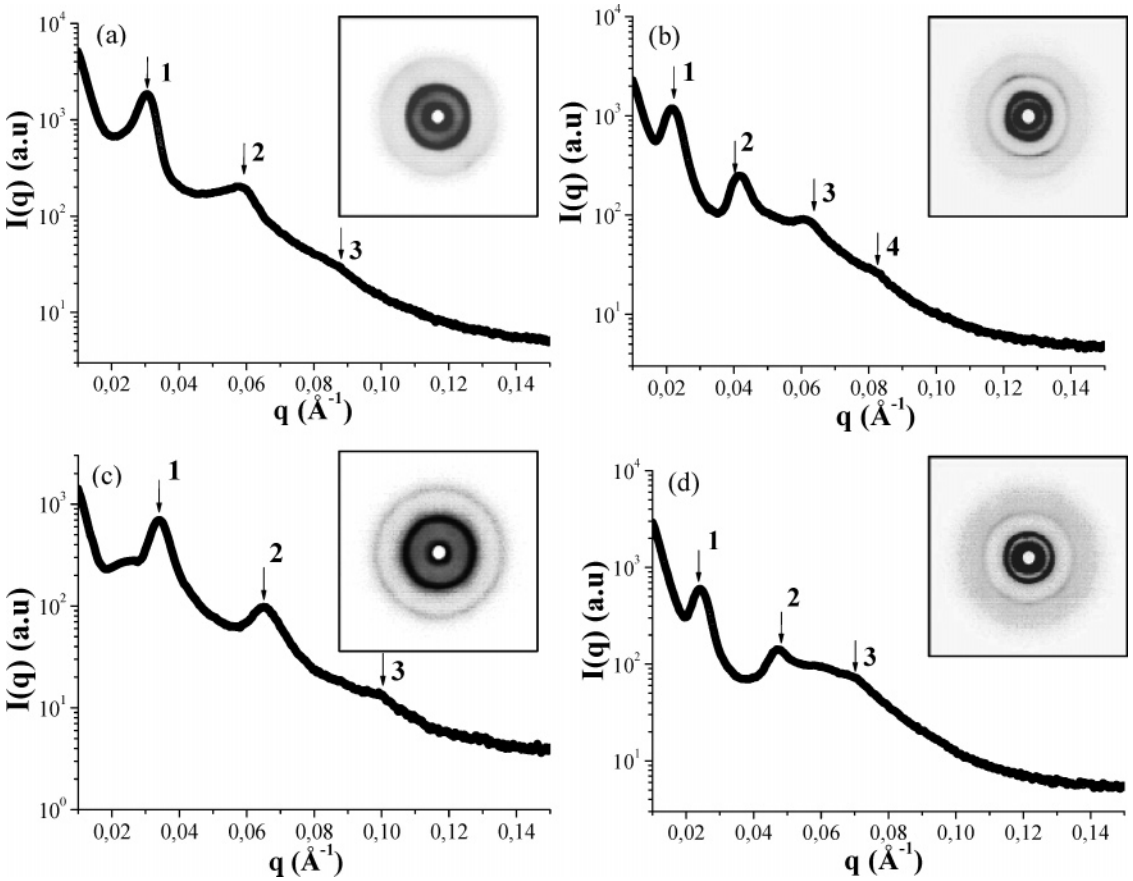

Figure 7. 1-D and 2-D SAXS patterns for, (a) PS_{24}-*b*-$PBLG_{76}$ (L2), (b) PS_{24}-*b*-PGA_{138} (L4), (c) PS_{24}-*b*-$(PGA_{36})_2$ (M2), and (d) PS_{24}-*b*-$(PGA_{71})_2$ (M4) copolymers.

the distance between neighboring helices (i.e diameter of PGA helices) was calculated as $d_\alpha = 4\pi/q^*\sqrt{3}$ (Table 2). For all copolymers a similar d_α value (16 Å) was obtained denoting no apparent effect of the copolymer architecture on the local organization of the polypeptide segment. Finally, the broad amorphous peak at $q^{**} = 1.48$ Å^{-1} with a corresponding average distance of 4.3 Å is correlated to aromatic interactions between amorphous polystyrene segments.

Next, small-angle X-ray scattering (SAXS) experiments were performed to determine the morphologies on a larger scale induced by the phase separation between PS and PGA. Representative SAXS patterns from linear diblock copolymers L2 and L4 and miktoarm star M2 and M4 analogues are shown in Figure 7. Whatever their composition and architecture, all block copolymers showed at least three peaks with a characteristic spacing ratio of 1:2:3, which is indicative of a lamellar morphology of alternating PS and PGA layers. These SAXS results combined with those obtained by FTIR on the local organization of the PGA α-helices allow us to conclude that the global structure adopted by the amphiphilic PS-*b*-$(PGA)_{n=1;2}$ copolymers is the hexagonal in lamellar (HL) morphology. This HL structure has been already observed on polyvinyl-*b*-polypeptide-protected PBLG and poly(ϵ-benzyloxycarbonyl-L-lysine) (PZlys) linear diblocks[27,33,35,36] and for PBLB-*b*-polyglycine copolypeptides.[60] Previous work on polypeptide based rod−coil copolymers revealed only one broad peak at low scattering angles,[33,35,36,61] characterizing a poorly ordered lamellar organization. More precisely, Schlaad et al.[35] attributed the presence of this single peak to an undulated lamellar or zigzag morphology induced by the hexagonal packing of polydisperse rodlike polypeptides (polydispersity ≈ 1.3) within the layers. In contrast, we observed three or four lamellar

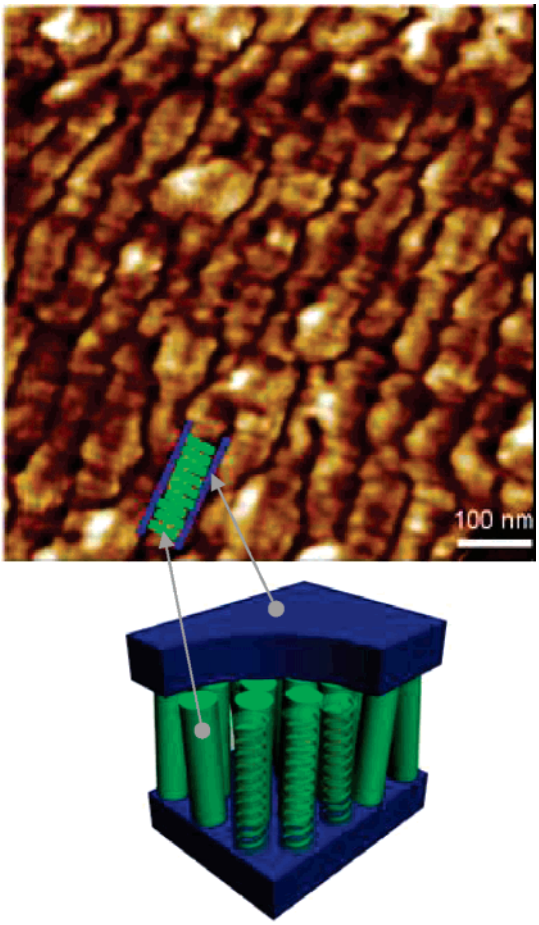

Figure 8. AFM image in phase mode of the self-assembled lamellar structure of a PS_{24}-*b*-$(PGA_{71})_2$ (M4) miktoarm star in the bulk; the inset/scheme represents the "hexagonal in lamellar" HL morphology.

scattering orders in our SAXS patterns suggesting a highly ordered lamellar organization. This can be attributed to the low polydispersity of our block copolymers on the basis of our synthetic methodology (Scheme 1). Gallot et al.[27,30−32] reported a similar highly ordered lamellar phase from nearly monodisperse PS-*b*-PBLG block copolymers obtained, however, after fractionation.

The hierarchical HL structure was confirmed by AFM measurements, which were directly performed on thick films used for WAXS/SAXS experiments; as illustrated in Figure 8. The phase-mode AFM image of the bulk samples of M4 shows a characteristic lamellar organization. The PS and PGA blocks are characterized by different mechanical properties, the PS block being soft (with a glass transition temperature around 50 °C) and the PGA block being more rigid because of hydrogen bonding between helices. As a consequence, we expect a characteristic phase contrast in the AFM phase-mode image between the PS and the PGA domains. Such a contrast is indeed observed in Figure 8. In addition, because of the larger volume fraction of the PGA block in the copolymer, we attribute the larger bright stripes to the PGA lamellae and the narrow and dark lines to the PS domains between successive PGA lamellae. The edges of these PGA domains are not straight but fluctuate significantly. This lamellar tapering may arise from the conjunction of (i) the molecular weight distribution of the PGA block and (ii) intralamellar segregation of the PGA blocks as a function of their molecular weight. Noteworthy, a similar lamellar tapering has been observed for rigid-rod conjugated polymers like polyfluorenes.[63,64] Within the lamellar PGA domains, one can also observe a substructure oriented roughly perpendicular

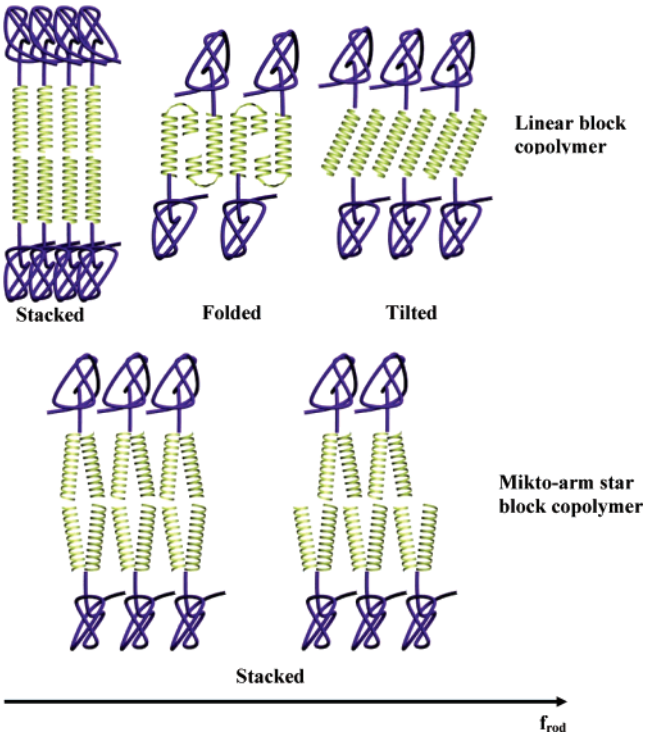

Figure 9. Schematic representation of the local packing of the PGA block as a function of the rod fraction for PS-*b*-PGA and PS-*b*-$(PGA)_2$ copolymers.

to the plane of the PGA lamellae. This latter substructure is most likely related to the tight packing of PGA α-helices in the lamellar domains. However, the size of the region explored herein did not allow us to distinguish between individual helices.

The presence of the lamellar morphology, no matter the composition and the architecture of the block copolymers, suggests that the self-assembly is mainly directed by the interaction of rigid PGA rods, forming anisotropic liquid-crystalline domains and planar interfaces. This behavior is markedly different from that of coil−coil copolymers where the phase separation is induced by the chemical incompatibility between each constitutive block, and which is controlled by the molecular weight, the volume fraction and the architecture of the coil−coil block copolymers. Our findings are in good agreement with theoretical phase diagrams of rod−coil diblock copolymers, where the lamellar structure exists independently of the block copolymer composition, except for highly asymmetric systems.[65−69] By analogy with liquid crystals, this lamellar structure can be viewed as a smectic A phase formed by a monolayer or a bilayer of rods, or as a smectic C phase where the rods are tilted compared to the layer orientation.[64] Even if the overall morphology of our self-assemblies does not seem to be affected by the composition and the architecture of the block copolymers, a refined analysis of SAXS data did show a significant impact of these parameters on the local packing of PGA helices within the lamellae (Table 2). A geometrical factor γ, introduced by Gallot et al.[27,31,32] and obtained by dividing the molecular volume of a chain by its average lateral extension (meaning the interfacial area per chain) and the cross section of a helix, can be used to clarify the polypeptide arrangement. For linear PS-*b*-PGA diblock copolymers, this factor γ depends on the block length ratio. For low polypeptide content, indeed, the PGA helices are stacked forming a bilayer ($\gamma = 1$ and $d_{PGA} = 2L_{PGA}$) while for higher content of PGA, helices are partially folded or tilted ($1 < \gamma < 2$ and $L_{PGA} < d_{PGA} < 2L_{PGA}$). As described by Schlaad,[34] local dipolar fields,

induced by the antiparallel orientation of the dipole moments (i.e., hexagonal packing of α-helices) limit the stability of helices, thus promoting a folding of the polypeptide segment when a critical polypeptide content is reached. In contrast, for PS-*b*-$(PGA)_2$ miktoarm stars, γ is independent of the composition and the PGA rods are always staked ($\gamma = 1$ and $d_{PGA} = 2L_{PGA}$) (Figure 9). This can be ascribed to the copolymer architecture and notably the presence of two PGA arms that probably prevents the folding of the polypeptide segments. In addition, the position of the branching point at the lamellar interface should induce a stretching of both the PGA and PS chains. The system should be able to relax such a constraint by increasing the interfacial curvature, provoking a morphological change. However, rod−rod interactions within the layers are the key driving forces responsible of the lamellar stabilization, confirming previous observations made on other constraint systems such as rod-dendrons.[12]

Conclusions

This is the first report on the self-assembly properties in bulk of linear PS-*b*-PGA and miktoarm star PS-*b*-$(PGA)_2$ block copolymers that were thoroughly characterized by FTIR, WAXS, SAXS, and AFM. Thick films were prepared by slow solvent evaporation thus reflecting self-assembled structures formed in the bulk and not at the surface of a thin drop-cast or spin-coated film, which excludes any segregation effect of the blocks at the film/air or substrate/film interfaces. To this aim, a novel four-step synthetic methodology was purposely developed to achieve block copolymers of well-controlled molecular weight and low polydispersity. The hydrophilic PGA block was found to systematically adopt a rigid rod conformation whatever its content in the block copolymer structure, whereas the PS part exhibits a coil conformation, as expected. All these rod−coil block copolymers displayed the hexagonal in lamellar (HL) morphology in the nanometer size range, independently of the composition and the architecture, reflecting the high incompatibility between the two blocks and the strength of the rod−rod interactions. The lamellar phase is even better organized than in most of the rod−coil block copolymers based on polypeptide reported so far. This can be correlated to the well-defined character of both linear and miktoarm star block copolymers based on PS and PGA at the molecular level on the basis of our controlled synthetic methodology. The PGA rigid block proved to play a major role toward nanophase separation by minimizing the effect of both the block length ratio and the branching point of miktoarm stars. The impact of the macromolecular architecture on the local organization of PGA helices was also evidenced: whereas for linear diblock copolymers the polypeptide segment can be folded or tilted at high PGA content, only stacked packing was observed for miktoarm star counterparts.

References and Notes

(1) Hamley, I. W. *The physics of block copolymers*; Oxford Science Publication: Oxford, U.K., 1998.
(2) Ciferri, A. *Supramolecular Polymers*; Marcel Dekker: New York, 2000.
(3) Leibler, L.; Orland, H.; Wheeler, J. C. *J. Chem. Phys.* **1983**, *79*, 3550.
(4) Bates, F. S. *Science* **1991**, *251*, 898.
(5) Fredrickson, G. H.; Bates, F. S. *Annu. Rev. Mater. Sci* **1996**, *26*, 501.
(6) Lodge, T. P. *Macromol. Chem. Phys.* **2003**, *204*, 265.
(7) Hadjichristidis, N.; Pispas, S.; Floudas, G. A. *Block Copolymers: Synthetic Strategies, Physical Properties, and Applications*; Wiley-Interscience: John Wiley & Sons, Inc., 2003.
(8) (a) Riess, G. *Prog. Polym. Sci.* **2003**, *28*, 1107. (b) Riess, G.; Labbe, C. *Macromol. Chem. Phys.* **2004**, *25*, 401.
(9) Klok, H. A.; Lecommandoux, S. *Adv. Mater.* **2001**, *13*, 1217.
(10) *Block Copolymers in Nanoscience*; Lazzari, M., Liu, G. G., Lecommandoux, S., Eds.; Wiley-VCH Verlag GmbH & Co., KGaA: Weinheim, Germany, 2006.
(11) Zubarev, R. E.; Pralle, M. U.; Sone, E. D.; Stupp, S. I. *J. Am. Chem. Soc.* **2001**, *123*, 4105.
(12) Lecommandoux, S.; Klok, H.-A.; Sayar, M.; Stupp, S. I. *J. Polym. Sci. Part A: Polym. Chem.* **2003**, *41*, 3501.
(13) Klok, H.-A.; Lecommandoux, S. *Adv. Mater.* **2001**, *13*, 1217.
(14) Lee, M.; Cho, B.-K.; Zin, W.-C. *Chem. Rev.* **2001**, *101*, 3869.
(15) Marko, J. F. *Macromolecules* **1993**, *26*, 1442.
(16) Borsali, R.; Minatti, E.; Putaux, J.-L.; Schappacher, M.; Deffieux, A.; Viville, P.; Lazzaroni, R.; Narayanan, T. *Langmuir* **2002**, *19*, 6.
(17) Iatrou, H.; Hadjichristidis, N.; Meier, G.; Frielinghaus, H.; Monkenbusch, M. *Macromolecules* **2002**, *35*, 5426.
(18) Thomas, E. L.; Alward, D. B.; Kinning, D. J.; Martin, D. C.; Fetters, L. J. *Macromolecules* **1986**, *19*, 2197.
(19) Nguyen, A. B.; Hadjichristidis, N.; Fetters, L. J. *Macromolecules* **1986**, *19*, 768.
(20) Taton, D.; Feng, X.; Gnanou, Y. *New J. Chem.* **2007**, *31*, 1097.
(21) Deffieux, A.; Schappacher, M. *Macromolecules* **1999**, *32*, 1797.
(22) Borsali, R.; Lecommandoux, S.; Pecora, R.; Benoît, H. *Macromolecules* **2001**, *34*, 4229.
(23) Crespo, J. S.; Lecommandoux, S.; Borsali, R.; Klok, H.-A.; Soldi, V. *Macromolecules* **2003**, *36*, 1253.
(24) Stupp, S. I.; LeBonheur, V.; Walker, K.; Li, L. S.; Huggins, K. E.; Keser, M.; Amstutz, A. *Science* **1997**, *276*, 384.
(25) Chen, J. T.; Thomas, E. L.; Ober, C. K.; Hwang, S. S. *Macromolecules* **1995**, *28*, 1688.
(26) Jenekhe, S. A.; Chen, X. L. *Science* **1999**, *283*, 372.
(27) Gallot, B. *Prog. Polym. Sci.* **1996**, *21*, 1035.
(28) Klok, H.-A.; Langenwalter, J. F.; Lecommandoux, S. *Macromolecules* **2000**, *33*, 7819.
(29) Lecommandoux, S.; Achard, M.-F.; Langenwalter, J. F.; Klok, H.-A. *Macromolecules* **2001**, *34*, 9100.
(30) Billot, J.-P.; Douy, A.; Gallot, B. *Makromol. Chem.* **1976**, *177*, 1889.
(31) Billot, J.-P.; Douy, A.; Gallot, B. *Makromol. Chem.* **1977**, *178*, 1641.
(32) Douy, A.; Gallot, B. *Polymer* **1982**, *23*, 1039.
(33) Babin, J.; Rodriguez-Hernandez, J.; Lecommandoux, S.; Klok, H.-A.; Achard, M.-F. *Faraday Discuss.* **2005**, *128*, 179.
(34) Schlaad, H.; Antonietti, M. *Eur. Phys. J. E.* **2003**, *10*, 17.
(35) Schlaad, H.; Smarsly, B.; Losik, M. *Macromolecules* **2004**, *37*, 2210.
(36) Schlaad, H.; Kukula, H.; Smarsly, B.; Antonietti, M.; Pakula, T. *Polymer* **2002**, *43*, 5321.
(37) Hadjichristidis, N.; Pispas, S.; Pitsikalis, M.; Iatrou, H.; Vlahos, C. *Adv. Polym. Sci.* **1999**, *142*, 71.
(38) Hadjichristidis, N.; Pitsikalis, M.; Pispas, S.; Iatrou, H. *Chem. Rev.* **2001**, *101*, 3747.
(39) Milner, S. T. *Macromolecules* **1994**, *27*, 2333.
(40) Grason, G. M.; Kamien, R. D. *Macromolecules* **2004**, *37*, 7371.
(41) (a) Pochan, D. J.; Gido, S. P.; Pispas, S.; Mays, J. W. *Macromolecules* **1996**, *29*, 5099. (b) Beyer, F. L.; Gido, S. P.; Velis, G.; Hadjichristidis, N.; Tan, N. B. *Macromolecules* **1999**, *32*, 6604. (c) Yang, L.; Hong, S.; Gido, S. P.; Velis, G.; Hadjichristidis, N. *Macromolecules* **2001**, *34*, 9069.
(42) Babin, J.; Leroy, C.; Lecommandoux, S.; Borsali, R.; Gnanou, Y.; Taton, D. *Chem. Commun.* **2005**, *15*, 1993.
(43) Gurkaynak, A.; Tubert, F.; Yang, J.; Matyas, J.; Spencer, J. L.; Gryte, C. C. *J. Polym. Sci., Part A : Polym Chem* **1996**, *34*, 349.
(44) For a recent highlight on ROP of *N*-carboxyanhydrides, see: Kricheldorf, H. R. *Angew. Chem., Int. Ed.* **2006**, *45*, 5752.
(45) Brzezinska, K. R.; Deming, T. J. *Macromol. Biosci.* **2004**, *4*, 566.
(46) Dong, C.-M.; Sun, X.-S.; Faucher, K. M.; Apkarian, R. P.; Chaikof, E. L. *Biomacromolecules* **2004**, *5*, 224.
(47) Dong, C.-M.; Faucher, K. M.; Chaikof, E. L. *J. Polym. Sci., Part A: Polym. Chem.* **2004**, *42*, 5754.
(48) Steig, S.; Cornelius, F.; Witte, P.; Staal, B. B. P.; Koning, C. E.; Heise, A.; Menzel, H. *Chem. Commun.* **2005**, 5420.
(49) Abraham, S.; Ha, C.-S.; Kim, I. *J. Polym. Sci., Part A: Polym. Chem.* **2006**, *44*, 4668.
(50) Abraham, S.; Ha, C.-S.; Kim, I. *J. Polym. Sci., Part A: Polym. Chem.* **2006**, *44*, 2774.
(51) Abraham, S.; Kim, I. Batt, C. A. *Angew. Chem. Int. Ed.* **2007**, *46*, 5720.
(52) Sinaga, A.; Ravi, P.; Hatton, T. A.; Tam, K. C. *J. Polym. Sci., Part A: Polym. Chem.* **2007**, *45*, 2646.
(53) Nicolas, J.; Mantovani, G.; Haddleton, D. M. *Macromol. Rapid Commun.* **2007**, *28*, 1083.
(54) Sen, A. C.; Keiderling, T. A. *Biopolymers* **1984**, *23*, 1533.
(55) Miyazawa, T.; Blout, E. R. *J. Am. Chem. Soc.* **1961**, *83*, 712.
(56) Lee, N. H.; Frank, W. C. *Langmuir* **2003**, *19*, 1295.
(57) Block, H. *Poly(γ-benzyl L-glutamate) and other glutamic acid containing polymers*; Gordon and Breach Science Publishers: New York, 1983.

(58) Papadopoulos, P.; Floudas, G.; Klok, H.-A.; Schnell, I.; Pakula, T. *Biomacromolecules* **2004**, *5*, 81.
(59) Wanatabe, J.; Uematsu, I. *Polymer* **1984**, *25*, 1711.
(60) Papadopoulos, P.; Floudas, G.; Schnell, I.; Aliferis, T.; Iatrou, H.; Hadjichristidis, N. *Biomacromolecules* **2005**, *6*, 2352.
(61) Ibarboure, E.; Rodriguez-Hernandez, J.; Papon, E. *J. Polym. Sci., Part A: Polym. Chem.* **2006**, *44*, 4668.
(62) P. S. *Gött Nachr.* **1918**, *2*, 98.
(63) Lieser, G.; Oda, M.; Miteva, T.; Meisel, A.; Nothofer, H.−G.; Scherf, U.; Neher, D. *Macromolecules* **2000**, *33*, 4490.
(64) Brinkmann, M. *Macromolecules* **2007**, *40*, 7532.
(65) Semenov, A. N.; Subbotin, A. V. *Sov. Phys. JETP A. V.* **1992**, *74*, 690.
(66) Williams, D. R. M.; Fredrickson, G. H. *Macromolecules* **1992**, *25*, 3561.
(67) Williams, D. R. M.; Halperin, A. *Phys. Rev. Lett.* **1993**, *71*, 1557.
(68) Matsen, M. W. *J. Chem. Phys.* **1996**, *104*, 7758.
(69) Reenders, M.; Brinke, G. T. *Macromolecules* **2002**, *35*, 3266.

MA702071Y